

## Microbial mediation in the formation of red limestones, Upper Carboniferous, Cantabrian Mountains, Spain

G. Della Porta<sup>1</sup>, B. Mamet<sup>2</sup> & A. Pr eat<sup>2</sup>

<sup>1</sup> Institut f ur Geowissenschaften, Universit at Potsdam, Postfach 601553, 14415 Potsdam, Germany; e-mail: della.porta@geo.uni-potsdam.de

<sup>2</sup> Universit e Libre de Bruxelles, Department of Earth and Environmental Sciences, 50, Avenue F.D. Roosevelt, CP 160/02, B-1050 Brussels, Belgium; e-mail: apreat@ulb.ac.be

### Abstract

The Bashkirian–Moscovian carbonate platform of the Sierra del Cuera (Cantabrian Mountains, N Spain) consists of 800–1000 m of horizontally-layered platform, bounded by a steep (20° to 40°) and high-relief (600–850 m) depositional slope. Slope clinoforms can be laterally traced downslope into the horizontal basin. The upper part of the slope (from the platform break downslope to nearly 300 m depth) consists of massive, microbial cement-rich boundstone with episodic intercalations of crinoidal packstones, bryozoan cement-rich accumulations and spiculitic wackestones with red micrite. The red layers (1–30 m thick) can be traced laterally for a few hundreds meters (from depth of 80 m to 400 m downslope of the platform break). On the platform top, metre-scale crinoidal packstones with red micrite are rare, but a layer 1–2 m thick can be laterally traced for at least 2 km.

The red colour is due to hematite that is concentrated in former cavities (bryozoan zoecia, foraminiferal chambers), within the network of crinoids, and in endolithic perforations within the macrofossils. Microbes are in the form of superficial coatings, or as straight and dichotomic filaments. Microscopical morphologies are ‘hedgehogs’, ‘blebs’ and stromatolites. Fungal hyphae are associated with omnipresent bacterial filaments.

As in other Paleozoic settings, the red colour is attributed to the presence of iron oxidizing bacteria and/or *fungi imperfecti*. The environments are relatively deep-water platform settings (likely a few tens of meters) and definitely deep parts (100 to at least 350 m) of the slope, below the storm wave base and below the photic zone. The process occurred in dysaerobic to anaerobic microenvironments below the sediment surface. The formation of hematite, which derived from probable former hydroxides, requires strong oxygen gradients.

This is the first described occurrence of red-stained deposits containing evidence of biological processes related to iron-oxidizing microbes that were deposited on a steep depositional slope fronting a high-relief carbonate platform.

*Keywords:* carbonate platform, Carboniferous, microbes, red limestones, Spain.

### Introduction

The Bashkirian–Moscovian carbonate platform of the Sierra del Cuera (Cantabrian Mountains, N Spain (Fig. 1) consists of 800–1000 m of a horizontally-layered platform, bounded by a steep (20° to 40°) and high-relief (600–850 m) depositional slope grading into a basin (Della Porta et al., 2002, 2003, 2004). The upper part of the slope, from the platform break to at least 300 m water depth, consists of microbial cement-rich boundstone. Massive boundstones are

episodically intercalated with lenses (1–30 m thick) of crinoidal packstones, skeletal and spiculitic wackestones and bryozoan radial fibrous cement-rich limestones with red-stained micrite in the wackestone portions. These red layers can be traced laterally for a few hundreds metres from water depth of 80 m downslope to 400 m with respect to the platform break (Della Porta et al., 2003, 2004).

This study examines these red layers with respect to the origin of the red colour of the micrite. The examination of the characteristics of the red layers

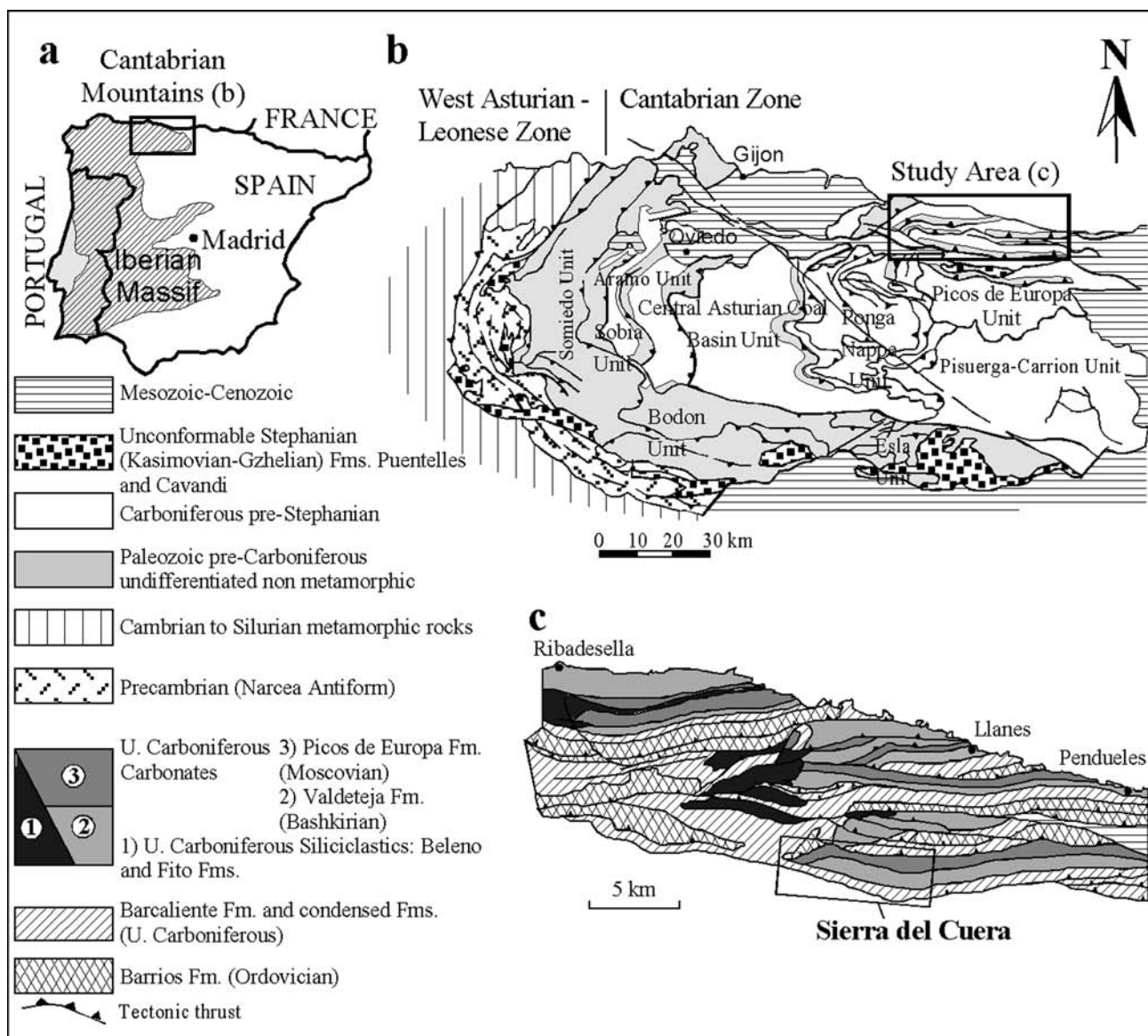


Fig. 1. Location of the Sierra del Cuera carbonate platform outcrop (a). Schematic geological map of the Cantabrian Zone (b) showing the different tectonostratigraphic Provinces/Units (modified after Julivert, 1971) and of the northeastern part of Ponga Nappe Unit ((c); modified after Bahamonde et al., 1997).

and the comparison with other Paleozoic and Mesozoic, recently studied, red limestones suggest that the red colour is linked to the presence of iron bacteria. Pioneer studies in the Frasnian 'Marbres Rouges' mud-mounds of the Ardennes (Belgium; Mamet & Boulvain, 1988; Boulvain, 1989, 1993; Boulvain et al., 2001) showed the presence of iron bacteria within the red-stained deposits. The red colour of the matrix could be attributed to the dispersal of submicronic hematite derived from the sheath of the iron bacteria. The same analyses were successively conducted in the Lower Carboniferous 'Griottes' of Asturias (Spain; Mamet & Boulvain, 1991) and in some Devonian 'Griottes' of the Central Pyrenees (Mamet & Perret, 1995). To test the hypothesis that the red colour was related to the presence of iron bacteria,

successive studies regarded also the Early Devonian Slivenec Limestone in Barrandium (Czech Republic; Mamet et al., 1997), the 'Griottes' of the Montagne Noire (France; Pr at et al., 1999a,b), the Mid-Jurassic of Normandy (France; Pr at et al., 2000), and the Jurassic Rosso Ammonitico of Italy (Mamet & Pr at, 2003).

All the observations, antecedent to the present work, examined red limestones located within carbonate platforms or in deep-water mud mounds and outer ramp settings. The iron was not of detrital origin and was linked to obvious bacterial activities in relatively deep-water sediments, including those deposited below or near the storm wave base and below the photic zone. This study aims to verify whether the interpretation of the bacterial origin of the red colour could be

extended to red deposits accumulated on a steep and high-relief carbonate-platform slope. This opportunity was offered by the red layers occurring within the slope deposits of the Upper Carboniferous Sierra del Cuera platform (Asturias, Spain). The depositional slope limits a several kilometre extensive carbonate platform and is adjacent to a basin at least 800–900 m deep. Slope deposits are continuously exposed and alternate with massive microbial cement-rich boundstone.

### Methods and materials

Eighteen samples collected on the slope red layers and two from the platform top red crinoidal packstones were examined through petrographic analysis of 55 thin sections and through scanning electron microscope. Biostratigraphic analysis on the basis of fusulinacean contents (Elisa Villa pers. comm.) indicated (a) a Late Bashkirian and (b) an Early Moscovian age, in agreement with the macrofossil assemblages (cf. Della Porta, 2003). Late Bashkirian (Zone 22) bioclasts in the slope red wackestones and packstones are partly reworked skeletal fragments from the platform top and include: Apterinellidae, *Ammoveritella* sp., *Asphaltina* sp., *Betpakodiscus* sp., *Biseriella* sp., *Calcisphaera* sp., *Calcitornella* sp., *Calcivertella* sp., *Climacammina* sp., *Donezella* sp., *Earlandia* sp., *Endothyra* sp., *Eolasiidiscus* sp., *Eostaffella* sp., *Globivalvulinella* sp., *Hemidiscus* sp. (abundant), *Insolemtitheca* sp., *Monotaxinoides* sp., *Neoarchaediscus* sp. (abundant), *Palaeotextularia* sp., *Profusulinella* sp., *Pseudoglomospira* sp., *Stacheoides* sp., *Tetrataxis* sp., and *Tuberitina* sp. Associated macrofossils include bryozoans and sponges, few brachiopods, molluscs, and trilobites. Fenestellid bryozoan cementstones are commonly interlayered with the red wackestones and packstones (Della Porta et al., 2003, 2004).

Early Moscovian bioclasts (Zone 23 or younger) in slope reworked red packstone and in platform bioclastic packstones and grainstones include: *Anchicodium* sp., *Calcivertella* sp., *Climacammina* sp., *Cuneiphyucus* sp., *Donezella* sp., *Endothyra* sp., epimastoporids, *Fourstonella* sp., *Neostafella* sp., *Planoendothyra* sp., *Pseudoglomospira* sp., *Tetrataxis* sp., *Tuberitina* sp., associated with abundant red algae such as *Komia* sp., *Ungdarella* sp., and *Ungdarellina* sp.

### Description and interpretation of the microscopic morphology of the iron constructions

The observed iron constructions are listed below (morphologies 1–12) and are schematically illustrated

in Fig. 2 (morphologies 1–11). Standard microscopy and SEM images of these morphologies (1–12) are represented in Plates 1 & 2. The iron-coated filaments show diameters of 0.5 to 2  $\mu\text{m}$ .

1. Bryozoan zoecia and foraminiferal chambers (e.g. in *Tetrataxis*, *Neoarchaediscus*, *Profusulinella*) with red intraparticle fillings and/or Fe-replacement.
2. Echinoderm fragments with irregular structures (possibly attributed to dissolution of calcite) and different stages of Fe-replacement of the former calcitic lattice.
3. Replaced intergranular coatings of former aragonite crystals.
4. Single or symmetrical coatings (possibly representing biofilms) on various substrates (ostracods, brachiopods, bryozoans).
5. Fillings of endolithic perforations that possibly were formed by algae, sponges, bacteria and fungi. The common recrystallization of the micritic fillings exhibits ‘rounded’ microspar.
- 6, 7. Specific large-scale morphologies derived from morphology 5: ‘hedgehog’ perforations (6) surrounded by hair-like single, dichotomic, or curved bacterial filaments, and more complex ‘cactus-like’ perforations (7).
- 8, 9. Blisters (8) and multiple blisters on crusts (9).
10. Incipient microstromatolites.
11. Hair-like single, dichotomic, straight and curved individual bacteriomorph filaments in matrix.
12. Ferruginous microfissures cutting all previous structures (matrix and cement).

Many bioclasts, with exception of bryozoans and brachiopods, are reworked from the platform top or areas upslope. Reworking is not indicated by extensive erosion but by a succession of chemical-physical events that occurred in various environments. Endothyrid foraminifers, which normally are abundant in the euphotic zone, are evidently weathered. Endothyrid walls are dissolved, transformed into a ‘fuzzy’ microspar and mud-filled. Iron introduction is following the micrite filling. Some irregular cavities are ultimately filled by transparent granular microspar and radiaxial fibrous cement. Similar complicated diagenetic sequences can be observed within some bryozoans, brachiopods, ostracods, kamaenid and donezellid algae.

The iron formation is interpreted to be of late origin, post-dating the carbonate sedimentation. For instance, reworked clasts of grey microbial boundstone are coated by fragile iron bioconstructions (mi-

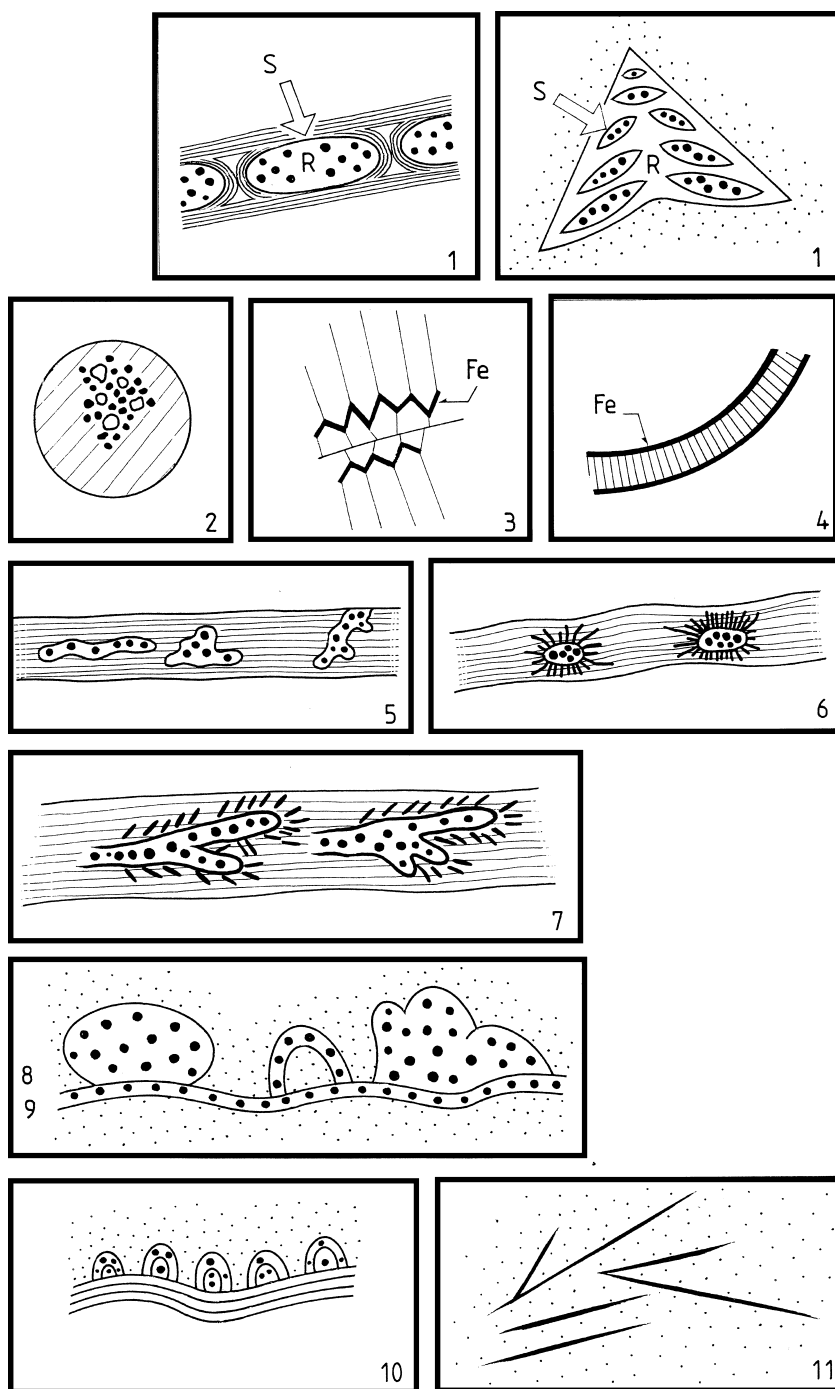


Fig. 2. Schematic representation of the distribution of the hematite within the analyzed red limestones. Refer to the text for explanation of the eleven figures. S = sediment (micrite), R = red iron infiltration interpreted as microbially induced. Arrows indicate strong gradients between Fe-poor sediment and Fe-enriched fillings (large dots). Irregular 'rounded' white dots are 'rounded' microspar.

crostromatolites, blisters) that are growing in the surrounding matrix. These coatings would not have withstood transportation and therefore are considered post-matrix infiltration.

A late phase of dissolution of the described fer-ruginized structures led to the formation of voids ultimately filled by transparent blocky calcite (or dolomite).

As shown in Plate 2 (figs 4–7, 10) the iron-coated filaments display diameters of 0.5 to 2  $\mu\text{m}$ . Some

of them are partly dichotomous and constitute assemblages of microtufts. As for the Devonian of the Montagne Noire (Préat et al., 1999b) and Belgium (Boulvain et al., 2001), these filaments have been interpreted as microbes that are morphologically similar to the Recent *Beggiatoales* (cf. Gillan & De Ridder, 1997). In addition, filaments attributable to bacteria with well preserved sheaths encrusted by hematite have been identified by SEM analyses (Plate 2, figs 4–5). Fungi, which have commonly larger size (Préat &

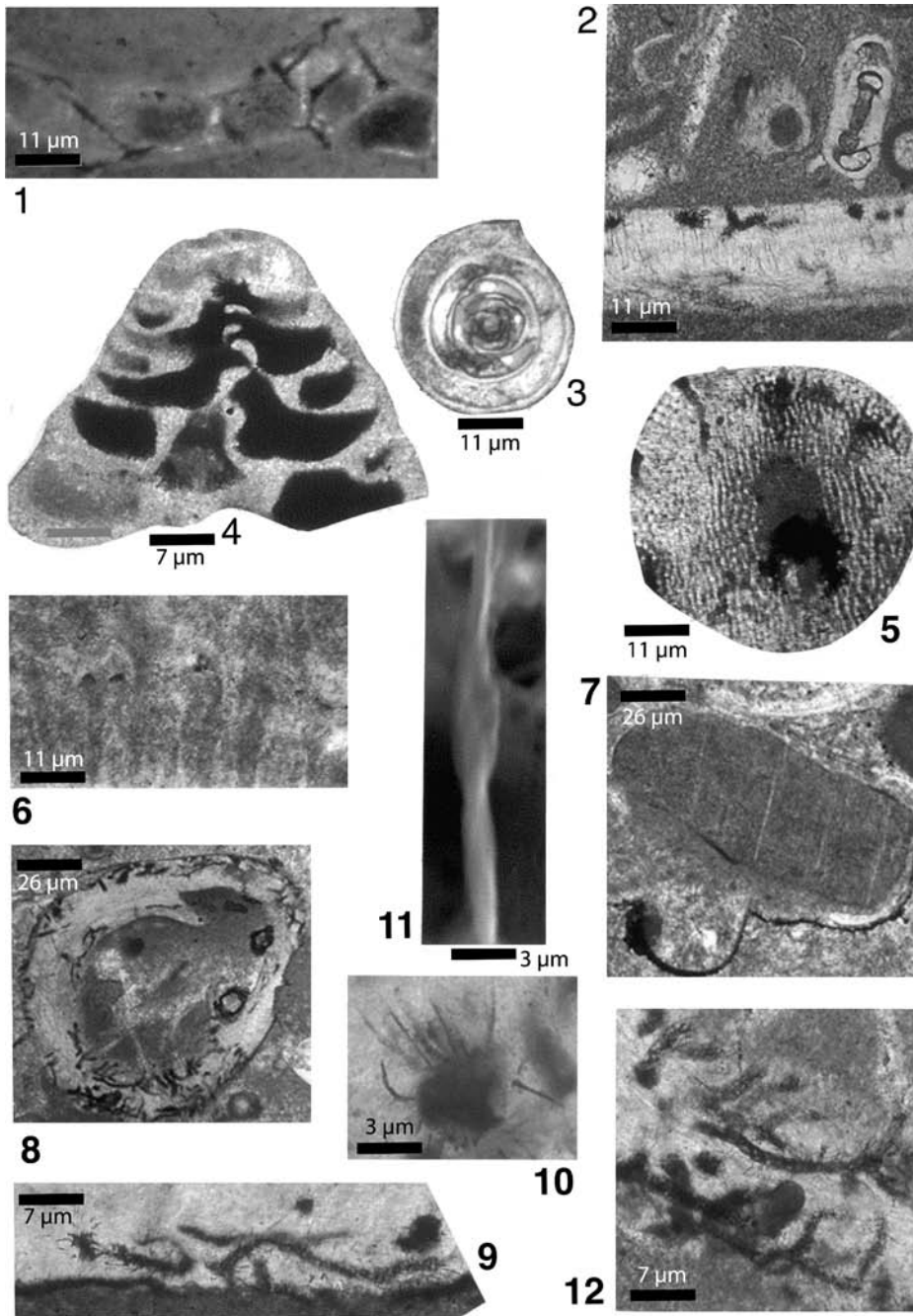


Plate 1. Morphologies 1–12 are those illustrated and summarized in Fig. 2. To notice that the images are slightly misleading as some iron fillings appear to be massive while they are instead filament coated. 1: Mud-filled bryozoan zoecia with variable hematitization (morphology 1). Strongly encrusted endolithic perforations (morphology 5). Sample 04-8, 150 m below the platform break, Late Bashkirian,  $\times 89$ . 2: Archæidiscid in a skeletal wackestone. The foraminifer has an uneven hematitized micrite filling (morphology 1) and a single continuous internal biofilm (morphology 4). A brachiopod has endolithic perforations (morphology 5) and scattered hedgehogs (morphology 6). Sample SC8B-88.0, 350 m below the platform break, Late Bashkirian,  $\times 89$ . 3: Archæidiscid with uneven hematitized filling (morphology 1), single continuous biofilm (morphology 4), internal sediment and evidence of dissolution of the wall. Sample 04-200C, same as fig. 1,  $\times 89$ . 4: Unevenly hematitized recrystallized *Terrataxis* (morphology 1). Sample 04-115, as fig. 1,  $\times 144$ . 5: Disintegration of crinoid ossicle possibly due to dissolution with Fe-filling of the original lattice (morphology 2). Some perforations are present at the periphery (morphology 5). Sample 04-190, as fig. 1,  $\times 89$ . 6: Coating of former aragonite crystals with hematite concentrated at tips of crystals (morphology 3). Sample 04-8, as fig. 1,  $\times 89$ . 7: Uneven Fe-crust in matrix (morphology 9). The echinoderm ossicles is surrounded by relict single biofilm (morphology 4). Sample SC8-74.5, as fig. 2,  $\times 36$ . 8: Extensive development of hematitized endolithic perforations (morphology 5). Remnants of peripheral biofilm (morphology 4); some internal blisters (morphology 8). Sample 04-190d, as fig. 1,  $\times 36$ . 9: Contact between sediment and a bryozoan underlined by a continuous biofilm (morphology 4). Endolithic filaments within recrystallized ‘rounded’ microspar (morphology 5). Various hedgehogs (morphology 6) surrounded by hair-like single filaments. Sample 04-130, as fig. 1,  $\times 144$ . 10: Hedgehog (morphology 6) surrounded by straight and curved filaments. Sample 04-190, as fig. 1,  $\times 288$ . 11: SEM illustration of a hematitized single filament surrounding a hedgehog. Sample SC8B-88.0, as fig. 2,  $\times 12000$ . 12: Endolithic perforation in a bryozoan with recrystallized ‘rounded’ microspar (morphology 5). Complex ‘cactus’ structure (morphology 7). Sample 04-190d, as fig. 1,  $\times 144$ .

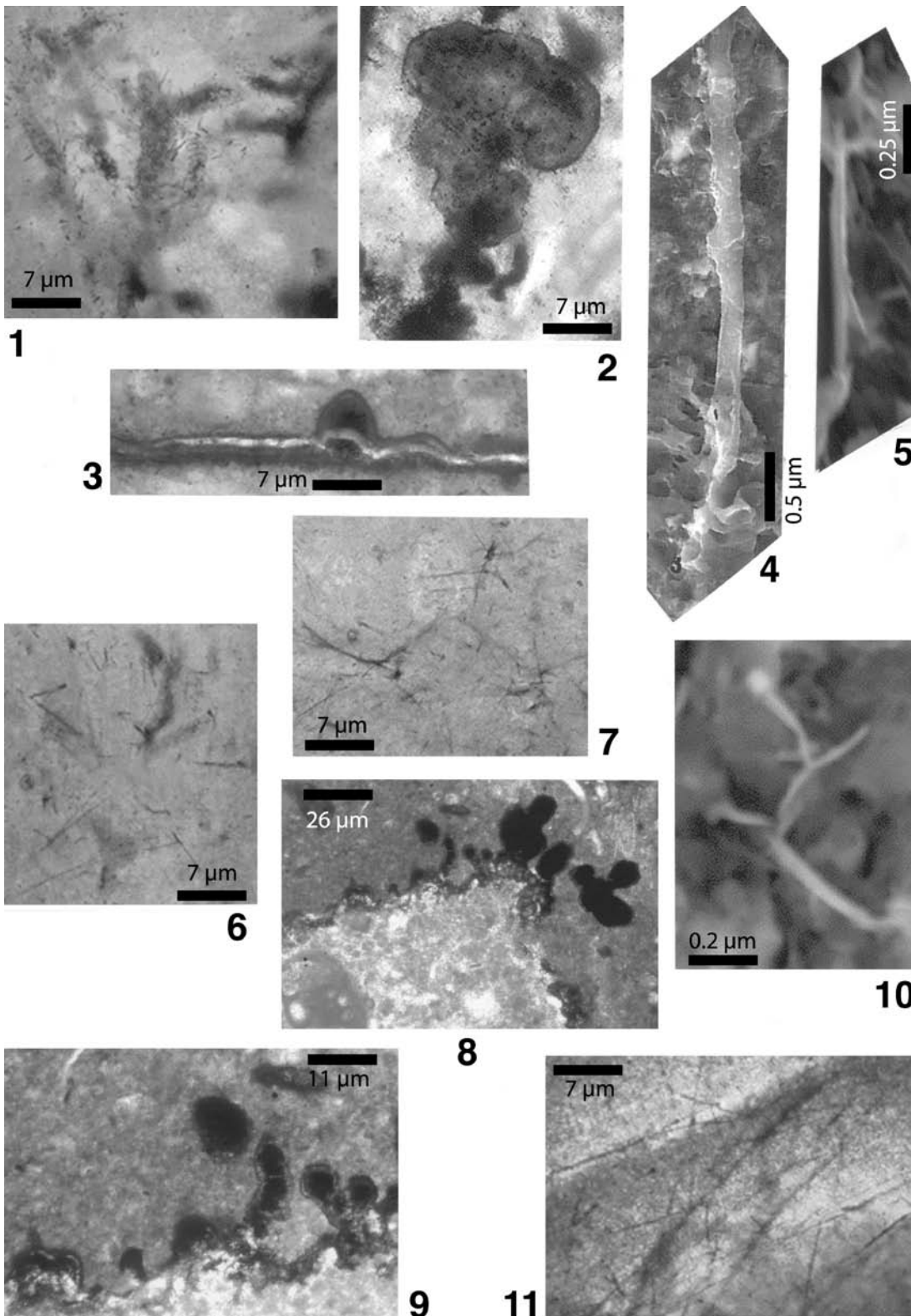


Plate 2. 1: Complex perforations (morphology 7) surrounded by numerous straight hematitized filaments ('cactus'). Sample SC8-88.0, 350 m below the platform break, Late Bashkirian,  $\times 144$ . 2: Multiple hematitized blisters (morphology 8). Sample RL07-CB, 450 m below the platform break, Early Moscovian,  $\times 144$ . 3: Simple blister (morphology 8) on a heavy hematite crust (morphology 9) with a continuous calcite string. Sample RL07-CB, same as fig. 2. 4-5: SEM picture of hematitized single and complex bacterial filaments surrounding a 'cactus' illustrated in fig. 1. Sample SC8B-88.0, as fig. 1,  $\times 2500$ ,  $\times 4000$  respectively. 6-7: Dichotomous radiating filaments within the matrix of the same sample (morphology 11). Sample SC8B-88.0, as fig. 1,  $\times 144$ . 8-9: (8) Small block of reworked recrystallized wackestone clast. Completely surrounded by incipient stromatolites (morphology 10) and blisters (morphology 8) growing in the surrounding red matrix. (9) Enlargement of the previous figure showing hematite/calcite layers. Sample SC8-79.0, 350 m below the platform break, Late Bashkirian,  $\times 36$  and  $\times 89$ , respectively. 10: SEM illustration of dichotomic iron-coated filament (morphology 11). Sample SC8-88B, as fig. 1,  $\times 5000$ . 11: Late ferruginous microfissures criss-crossing previous structures (morphology 12). Sample SC8-85, as fig. 1,  $\times 144$ .

Gillan, 2004), seem not to be present in the studied material of Asturias.

### Comparison with previously studied red limestones and discussion

Previously studied red limestones (see Introduction), where the reddish colour has been attributed to iron bacterial activity on the basis of SEM identifiable iron-clad filaments, exhibited also morphologies recognizable by petrographic analysis remarkably similar to those observed in the present study. These morphologies include: (1) iron filling of original cavities in macrofossils; (2) Fe-replacement of calcitic matrix in such cavities; (3) endolithic perforations, preferentially Fe-coated, forming 'hedgehogs' and 'cactuses'; (4) single coating (possible biofilm) at the base or upper surface of substrates (usually a macrofossil); (5) multiple coatings (biofilms) usually separated by calcite stringers; (6) multiple laminated structures (possible biofilms) forming microstromatolites that must have been nonphototropic (e.g., not related to cyanobacteria) because they formed within dark cavities or at the lower surface of the substrate; (7) dispersion of iron in the carbonate matrix; (8) late concentration of iron in stylolites or in fissures criss-crossing the sediment; (9) later dissolution of marine calcite into voids and late dolomitic cement. These events are not always observed in the same temporal sequence, but they are common to all studied limestones listed in the Introduction paragraph.

It is suggested that the iron microbial activity is responsible for the red pigmentation of the matrix owing to the bioprecipitation of submicronic iron/manganese oxy-hydroxide minerals in microaerophilic conditions at dysoxic-anoxic water-sediment interfaces (Ghiorse, 1984; Pr at & Gillan, 2004) where the observed iron bioconstructions grew (see Fig. 2). This has also been suggested for the red Devonian limestones (Pr at et al., 1999a,b; Boulvain et al., 2001). The former iron oxy-hydroxides could have been quickly transformed in hematite over a period of weeks to months (Cornell & Schwertmann, 1996). In fact, the iron formation exhibits evidences of post-dating the carbonate sedimentation. This process took place during the early diagenesis at the sediment-water interfaces where oxygen gradients were still present.

Red carbonates where the colour can be linked to the iron-bacterial activity have comparable paleogeographic interpretation. They were formed within relatively deep-marine sediments deposited below the fair weather wave base and sometimes below the storm wave base and the dysphotic-aphotic zone boundary, in calm conditions with low oxygen and fer-

rous iron concentrations. Below the storm wave base, red coloured limestones have no precise bathymetric significance. By using modern analogues (Budd & Perkins, 1980; Perry & MacDonald, 2002), red limestones can be formed anywhere in marine water below 80–100 m. Red limestones have been observed in the Paleozoic and Mesozoic time intervals, in deep-water settings at the top of carbonate platforms (this study), in mud-mound accumulations, in hemipelagic deposits in the outer part of low-angle carbonate ramps and in steep, high-relief slopes (this study). The deep-water occurrences of red limestones could explain the red colour of bathyal sediments such as the silicified red radiolarites (lydites).

### Conclusions

The red layers of the Sierra del Cuera platform form 1–30 m thick units that were deposited on a steep (20–30°), high-relief slope at depths of 80–400 m. The red layers consist of spiculitic wackestones, crinoidal packstones and bryozoan cement-rich limestones and alternate with microbial cement-rich boundstone. On the platform top, red crinoidal packstones are rare, 1–3 m thick and are indicative of events of rapid flooding and deeper water-depth conditions of platform deposition. Slope and platform red limestones contain iron structures and constructions that can be morphologically attributed to microbial (possibly iron-bacteria) activity. On the slope the environment was deep, dysphotic-aphotic, low energy and with oxygen gradients. These conditions might have favoured the iron-bacterial activity as it has been observed in other Paleozoic and Mesozoic red limestones. This is, however, the first recorded case of red layers on a steep slope facing a 850 m-deep basin. The, bacterially induced, red colour might explain the red colour of silicified radiolarites in bathyal settings.

### References

- Bahamonde, J.R., Colmenero, J.R. & Vera, C., 1997. Growth and demise of late Carboniferous carbonate platforms in the eastern Cantabrian Zone, Asturias, northwestern Spain. *Sedimentary Geology* 110: 99–122.
- Boulvain, F., 1989. Origine microbienne du pigment ferrugineux des monticules micritiques du Frasnien de l'Ardenne. *Annales de la Soci t  g ologique de Belgique* 112: 79–86.
- Boulvain, F., 1993. S dimentologie et diagen se des monticules micritiques du 'F2j' du Frasnien de l'Ardenne. *Professional Paper* 260. Service g ologique de Belgique: 427 pp.
- Boulvain, F., De Ridder, Ch., Mamet, B., Pr at, A. & Gillan, D., 2001. Iron microbial communities in Belgian Frasnian carbonate mounds. *Facies* 44: 47–60.
- Budd, D.A. & Perkins, R.D., 1980. Bathymetric zonation and paleoecological significance of microboring in Puerto Rican and

- shelf slope sediments. *Journal of Sedimentary Petrology* 50(3): 881–904.
- Cornell, R.M. & Schwertmann, U., 1996. *The Iron Oxides: Structure, Properties, and Uses*. UCH Weinheim, Germany.
- Della Porta, G., Kenter, J.A.M., Immenhauser, A. & Bahamonde, J.R., 2002. Lithofacies character and architecture across a Pennsylvanian inner-platform transect (Sierra de Cuera, Asturias, Spain). *Journal of Sedimentary Research* 72(6): 898–916.
- Della Porta, G., 2003. Depositional anatomy of a Carboniferous high-rising carbonate platform (Cantabrian Mountains, NW Spain): Published PhD Thesis, Vrije Universiteit (Amsterdam, The Netherlands): 250 pp.
- Della Porta, G., Kenter, J.A.M., Bahamonde, J.R., Immenhauser, A. & Villa, E., 2003. Microbial boundstone dominated carbonate slope (Upper Carboniferous, N Spain): microfacies, lithofacies distribution and stratal geometry. *Facies* 49: 175–208.
- Della Porta, G., Kenter, J.A.M. & Bahamonde, J.R., 2004. Depositional facies and stratal geometry of an Upper Carboniferous prograding and aggrading high-relief carbonate platform (Cantabrian Mountains, N Spain). *Sedimentology* 51: 267–295.
- Ghiorse, W.C., 1984. Biology of iron and manganese-depositing bacteria. *Annales de la Revue Microbiologie* 38: 515–550.
- Gillan, D. & De Ridder, Ch., 1997. Morphology of ferric iron-encrusted biofilm forming on the shell of a burrowing bivalve (Mollusca). *Aquatic Microbial Ecology*, 12: 1–10.
- Julivert, M., 1971. Décollement tectoniques in the Hercynian cordillera of northwest Sapin. *American Journal of Science* 270: 1–29.
- Mamet, B. & Boulvain, F., 1988. Remplissages bactériens de cavités biohermales frasnienues. *Bulletin Société belge de Géologie* 97(1): 63–76.
- Mamet, B. & Boulvain, F., 1991. Constructions hématitiques de griottes carbonifères (Asturies, Espagne). *Bulletin Société belge de Géologie* 99(1): 229–239.
- Mamet, B. & Perret, M.F., 1995. Bioconstructions hématitiques de griottes dévoniennes (Pyrénées Centrales). *Géobios* 28(6): 655–661.
- Mamet, B. & Préat, A., 2003. Sur l'origine bactérienne et fongique de la pigmentation de l'*Ammonitico Rosso* (Jurassique, région de Vérone, Italie du Nord). On the bacterial and fungal origin of the Ammonitico Rosso red pigmentation (Jurassic, Verona area, northern Italy). *Revue de Micropaléontologie* 46: 35–46.
- Mamet, B., Préat, A., & De Ridder, Ch., 1997. Bacterial origin of the red pigmentation in the Devonian Slivenec Limestone, Czech Republic. *Facies* 36: 173–188.
- Perry, C.T. & MacDonald, I.A., 2002. Impacts of light penetration on the bathymetry of reef microboring communities: implications for the development of microendolithic trace assemblages. *Paleogeography, Paleoclimatology, Paleoecology* 186(1–2): 101–113.
- Préat, A. & Gillan, D. 2004. Activités microbiennes (ferro-bactéries et *fungi*) et origine des matrices carbonatées rougeâtres au Paléozoïque. In Préat et al. (eds): *Ecole d'Été des Carbonates récifaux et de plate-forme*, Université de Grenoble, Publication Spéciale Association des Sédimentologues Français: 24–33.
- Préat, A., Mamet, B., Bernard, A. & Gillan, D., 1999a. Rôle des organismes microbiens dans la formation des matrices rougeâtres paléozoïques: exemple du Dévonien, Montagne Noire. *Revue de Micropaléontologie* 42(2): 161–182.
- Préat, A., Mamet, B., Bernard, A. & Gillan, D., 1999b. Bacterial mediation, red matrices diagenesis, Devonian, Montagne Noire (southern France). *Sedimentary Geology* 126: 223–242.
- Préat, A., Mamet, B., De Ridder, Ch., Boulvain, F. & Gillan, D., 2000. Iron bacterial and fungal mats, Bajocian stratotype (Mid-Jurassic, northern Normandy, France). *Sedimentary Geology* 137: 107–126.